Molecular dynamics simulation of induced anisotropy. I. Equilibrium properties

M. W. Evans

Chemistry Department, University College of Wales, Aberystwyth, Dyfed, SY23 1NE, Wales
(Received 10 March 1981; accepted 22 June 1981)

A simple mechanical torque is applied to 108 C_{2v} triatomics in a molecular dynamics computer simulation. The effect of the torque on equilibrium autocorrelation functions is evaluated for vectors of interest to the analytical theory of molecular diffusion in anisotropic liquids. The results of the simulation do not, in general, support the conventional viewpoint based on Debye's theory of rotational diffusion. In particular, the angular momentum acf becomes more oscillatory in the anisotropic liquid, which is not the case in theories of liquid anisotropy such as those of Bénoit, Ullman, and others in the literature.

I. INTRODUCTION

The liquid phase of matter is usually isotropic at equilibrium. Properties such as the complex permittivity and refractive index are identical if measured along mutually orthogonal directions X, Y, and Z in the laboratory frame. This ceases to be the case when the sample is treated with a more or less intense field of force applied along one of these axes, say Y. It is well known that birefringence is observable[1] in a liquid treated with an intense electric field (the Kerr effect), magnetic field (the Faraday or Cotton/Mouton effect), or laser field. Denoting the refractive index change by Δn, the ratio $\Delta n/n$ is usually very small in normally isotropic liquids of measurable index n. In the alignment of mesophases, the mutual coordination on the molecular scale results in $\Delta n \doteqdot n$ with relatively weak aligning fields (electric or magnetic).

The theory of molecular diffusion in anisotropic liquids is based[2] on equations which govern the evolution with time of probability density functions under the influence of an applied force or torque. The first detailed publication seems to be that of Bénoit,[3] who bases his treatment on Debye's theory of rotational diffusion, with the basic assumption that in energy terms the external perturbation is much smaller than the thermal kT. In this case $\Delta n \ll n$ and the rise and fall transients $\Delta n(t)/n$ mirror each other, i.e., are contemporaneous and have the same shape. Ullman[4] has more recently extended the theory to deal with an applied torque whose energetic effect exceeds kT. This author provides results for energetic perturbations of as much as $10kT$. In general, however, the standard theoretical approach is based on a stochastic differential equation such as the one used by Coffey and Paranjape[5]:

$$\frac{2\tau\partial f(\theta,t)}{\partial t} = \frac{1}{\sin\theta}\frac{\partial}{\partial\theta}\left\{\sin\theta\left[\frac{\partial f(\theta,t)}{\partial\theta} - \frac{f(\theta,t)M(\theta,t)}{kT}\right]\right\}. \quad (1)$$

This has also been used by Nordio *et al.*[6] as a basis for the molecular theory of liquid crystalline behavior. Equation (1) is written purely in isotropic configuration space (θ) for the variation of the probability density function $f(\theta, t)$ of a rigid dipole of moment μ undergoing purely rotational Brownian motion under the influence of a unidirectional external electric field $\mathbf{E}(t)$. $M(\theta, t)$ is the magnitude of the torque acting on the dipole due to $\mathbf{E}(t)$, and τ the Debye relaxation time.

Recently, Grigolini and co-workers[7] have extended the validity of this equation to the non-Markovian case where the field $\mathbf{E}(t)$ can become arbitrarily large. The increasingly abstract nature of the mathematics involved in this extension leads to the conclusion that a computer simulation of the induction of anisotropy should be carried out in order to extract a few of the many molecular averages of theoretical (and practical) interest. These include the rise and fall transients themselves, but of primary interest are autocorrelation functions such as those of molecular angular momentum or orientation. With arbitrarily strong external fields it is also necessary to know whether the fluctuation–dissipation theorem[8] is approximately valid when dealing with the rise transient, and to compare the development of rise and fall transients[1] for different strengths of extreme perturbation.

Firstly, however, it is as well to simulate the effect of an arbitrarily strong torque when the system has been allowed to come to equilibrium. This is the subject of part I of this series, where we use the technique of "molecular dynamics" simulation[8] to treat a liquid sample with an extra torque, reequilibrate, and compare the torque-on and torque-off equilibrium averages. A second paper will deal with a pulse of applied torque, equivalent to a square wave in the picosecond range, so that a direct simulation of the resulting rise and fall transients[1] is possible.

The paper is organized as follows: In Sec. II we describe the system in detail and explain the nature of our modeled external torque. In Sec. III the effect on the equilibrium properties such as total energy is monitored before proceeding in Sec. IV to describe the effect on molecular autocorrelation and response functions of interest. Finally, in Sec. V we consider how these results might be used to aid in clarifying the concepts behind the analytical theory.

II. THE ALGORITHM (UMRCC CDC 7600/1904S COMPUTER)

The algorithm used is based on that developed by Renaud and Singer[9] and called TRI2 by the authors. The equations of motion are integrated for 108 triatomic molecules of C_{2v} symmetry interacting with a 3×3 Lennard-Jones potential in a pairwise additive manner.

 0021-9606/82/115473-07$02.10

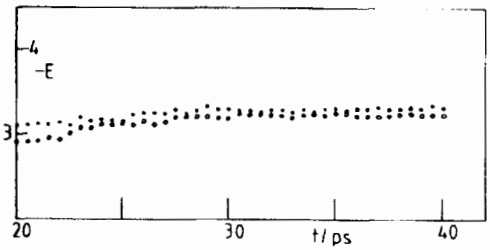

FIG. 1. Equilibrated total thermal energy (E) (in reduced units) from 20 to 40 ps. ●, Torque on; ○, torque off. Ordinate: $-10^{-5}E$; abscissa: time (ps).

The Lennard-Jones parameters for each atom are $\sigma = 3.0\times10^{-10}$ m and $\epsilon/k = 173.5$ K. The integrating algorithm is a predictor type with periodic boundary conditions and long-range potential cutoff. Labeling the molecule by ABC, the dimensions follow as AB = BC $= 10^{-10}$ m, $m_A = m_B = m_C = 2.5\times10^{-25}$ kg, and $\angle$ ABC = 60°. The C_{2v} structure of the molecular framework allows us to define three vectors $\mathbf{e}_A$, $\mathbf{e}_B$, and $\mathbf{e}_C$ along the I_A, I_B, and I_C moment of inertia axes of each molecule. The triatomic ABC bears some relation to a weakly dipolar nonpolarizable triatomic, but is otherwise not intended as a "real" molecule.

The thermodynamic conditions of the run are fixed by setting initially the temperature and molar volume at 220 K and 10^{-4} m^3, respectively. The temperature was allowed to fluctuate in the range ±25 K, and scaled, if necessary, every 50 time steps, i.e., every 0.5 ps. In preparation for a run in the equilibrium liquid state the molecules were deployed on a lattice which melted over the initial 20 ps. This process was monitored through the translational and rotational kinetic energy, the potential energy, total thermal energy, and virial. The total thermal energy eventually reaches its equilibrium plateau level, illustrated in Fig. 1. The external torque has no discernible effect on temperature scaling. This is necessary occasionally (every 1000 time steps or so) at "equilibrium" both in the torque-off and torque-on cases. The total thermal energy is maintained at the same level both in the torque-off and torque-on cases because the temperature is maintained constant by the thermostat (or temperature scaling). In addition to the thermal energy we have the total interaction energy $\sum_i \boldsymbol{\mu}_i(t)\cdot\mathbf{E}$. This is governed by a Langevin function and is dealt with in Sec. III. For the purpose of constructing autocorrelation functions from the dynamical data, the algorithm was restarted at the 20 ps mark, and run for another 20 ps (sometimes 30 ps), recording the data at 0.03 ps intervals onto nine track magnetic tape using the CDC 7600 mass storage facility. Autocorrelation functions of various kinds were then computed using separate algorithms based on running time averages. The stability of the results was checked by comparing averages over 10 and 20 ps intervals with 0.03 ps subintervals. One such check is illustrated in Fig. 9. The vectors in which we are interested are $\mathbf{v}$, the center of mass velocity, $\mathbf{J}$, the angular momentum, $\mathbf{T}_q$, the torque, that of the vector $\mathbf{e}_B$ (an orientation vector), and of $\dot{\mathbf{e}}_B = \mathbf{J}\times\mathbf{e}_B$, from which we construct the rotational velocity acf.[2,8] The latter is primarily useful as being the second derivative of $\langle\mathbf{e}_B(t)\cdot\mathbf{e}_B(0)\rangle$ and therefore a means of detailing its short time behavior, equivalent with the far infrared range of frequencies.

A second run was carried out under these conditions with the addition of an external torque $-\mathbf{e}_B\times\mathbf{F}_Y$ to that part of the algorithm used to calculate the resultant internal torque on each molecule at every time step. The magnitude of $\mathbf{T}_{ext}$ is 2.76×10^{-11} N. The extra torque vector therefore takes effect in a direction mutually orthogonal to both $\mathbf{e}_B$ and $\mathbf{F}_Y$, its magnitude being $-\mathbf{e}_B F_Y \sin\theta$, where θ is the angle between $\mathbf{e}_B$ and $\mathbf{F}_Y$ for each of the 108 molecules. We emphasize that our intermolecular potential does not contain electrodynamic terms (i.e., molecular electric field multipole–multipole interaction terms). However, the external torque would be electrical in origin if $\mathbf{e}_B$ were a dipole moment vector and $\mathbf{F}_Y$ an electric field strength vector. If we were to adopt a polarizable potential involving the molecular polarizability tensor $\boldsymbol{\alpha}$, we would have interaction terms[1] nonlinear in "electric field" strength $\mathbf{F}_Y$. Similarly, the Faraday effect could be simulated using the relevant magnetic terms. In the present case we confine our investigation to the simplest mechanism of anisotropy inducement in order to expose the essentials of the problems at hand: those caused by using an arbitrarily strong $\mathbf{F}_Y$. We propose to call the torque $\mathbf{T}_{ext} = -\mathbf{e}_B\times\mathbf{F}_Y$ a *mechanical* torque, in contrast to the electric torque of the Kerr effect, magnetic torque of the Faraday effect, electromagnetic (laser) torque, spin–dipole (NMR) torque, etc. We note that in an equation such as Eq. (1), the *precise origin* of $M(\theta, t)$ may be left out of consideration. For example, Eq. (1) has been used[6] as written when M stands for the magnitude of the nematic director torque rather than for the electric field induced torque magnitude of the Kerr effect.[3–5]

The equilibration process described above was repeated in the presence of $\mathbf{T}_{ext}$, keeping to the same temperature and molar volume. As a consequence of this thermostating, the total thermal energy plateau is the same with or without $\mathbf{T}_{ext}$. Autocorrelation functions and related averages were evaluated at equilibrium as above.

III. EQUILIBRIUM PROPERTIES

These are summarized in Table I, using the reduced units of the particular algorithm used. To convert from reduced units to S. I. units we use the following: Denote reduced units by an asterisk. Then, $\mathbf{r}^* = \mathbf{r}/H$, where r is length ($m$) and H half its box length; $\epsilon^* = \epsilon/H^2$, where

TABLE I. Effect of $\mathbf{T}_{ext}$ on equilibrium averages.

Vector	Ratio of equilibrium root mean square average value; torque on to torque off (running-time averaging technique)
$\mathbf{T}_q$	1.34
$\mathbf{J}$	0.99
$\mathbf{e}_B$	1

ϵ is the Lennard-Jones energy; $T_q^* = T_q^*/H^2$; $J^* = J/H^2$; $I^*_{A,B,C} = I_{A,B,C}/H^2$; $v^* = vt/H$, where v is the c.m. velocity and t the time step in secs.

The behavior of the total thermal energy during the equilibration process is illustrated in Fig. 2, with the external torque applied during the melt process. Eventually, the level falls to the negative plateau value of Fig. 1, i.e., to essentially the same level as in the absence of torque. The change in equilibrium thermal quantities brought about by the external torque is therefore small.

The change in the "statistical structure" of the system may be monitored using the test of Gaussian moments first used by Rahman[10] and taken up by Berne and Harp[11] and Evans *et al.*[8,12] These measure how well the concept of equilibrium Maxwell–Boltzmann statistics applies in the microcanonical ensemble under consideration. The Gaussian distribution is evaluated using their well known a_n functions ($n = 1, 2, 3, \ldots$) which all vanish in the Gaussian limit. In Table II some of our results are tabulated with and without the external torque. The a_n values are averages over the 20 ps of the run at 0.03 ps intervals. The spread in a_n is indicated by the standard deviation. The torque vector is again more significantly affected than the other two.

Finally, in this section on equilibrium properties we note the major structural changes brought about by the mechanical torque. This is manifested in the *anisotropy* of the equilibrium values of the dynamical vectors. The greatest effect is on the orientation vector $\mathbf{e}_B$, where we have $\langle e_{Bx}^2\rangle/\langle \mathbf{e}_B^2\rangle = 0.34$, $\langle e_{By}^2\rangle/\langle \mathbf{e}_B^2\rangle = 0.61$, and $\langle e_{Bz}^2\rangle/\langle \mathbf{e}_B^2\rangle = 0.33$. Strictly speaking, therefore, the sample becomes not birefringent but slightly trirefringent with this kind of external perturbation. It would probably be difficult to observe this experimentally under anything but the most favorable conditions, i.e., those allowing the use of a very intense pulse, of energetic effect comparable with kT. It follows from the anisotropy of the $\mathbf{e}_B$ and J averages that the anisotropy in the $\mathbf{e}_B$ averages is going to be very pronounced, so that the far infrared spectrum[2,8] should be a fairly sensitive means of investigating phenomena of this type.

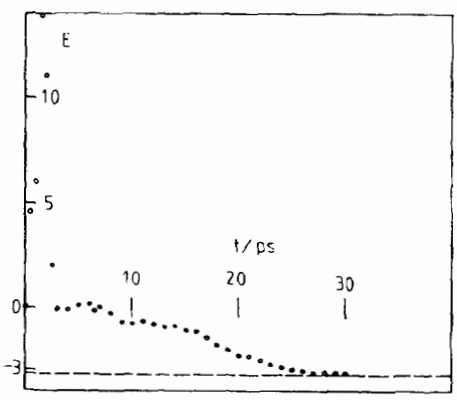

FIG. 2. Equilibration of the total thermal energy during the melting process with applied torque. Ordinate: total energy; abscissa: time (ps).

TABLE II. Non-Gaussian behavior with and without torque.[a]

Vector	Without			With		
	a_1	a_2	a_3	a_1	a_2	a_3
J	0.26 ± 0.15	0.83 ± 0.72	1.96 ± 2.41	0.22 ± 0.11	0.60 ± 0.41	1.15 ± 1.07
v	0.75 ± 0.27	2.55 ± 1.50	6.54 ± 6.57	0.77 ± 0.25	2.63 ± 1.40	6.71 ± 5.51
T_q	0.56 ± 0.32	2.19 ± 2.21	6.75 ± 11.70	0.22 ± 0.19	0.77 ± 1.01	2.01 ± 3.87

[a]± Standard deviation.

IV. AUTOCORRELATION FUNCTIONS AND RESPONSE FUNCTIONS

The purpose of this section is to simulate the effect of the perturbation $\mathbf{T}_{ext}$ on the various time autocorrelation functions (acf's) of theoretical interest. With longer runs it may be possible in the future to simulate the cross correlations as well.[13] The time acf's are equilibrium properties, and the fluctuation–dissipation theorem relates them to transient properties such as $\Delta n(t)/n$, the transiently induced birefringence. By this means, equations of motion on a molecular scale may be used to produce frequency domain spectra. A computer simulation in this context aids us in the evaluation of basic theoretical suppositions which link the analytical theory and raw spectra. It is well known by now[2,8] that Eq. (1), e.g., contains model assumptions which are supported neither by computer simulation nor by an analysis of, for example, far infrared spectra. If we attempt to extend Eq. (1) in a phenomenological way, following the methods of Grigolini *et al.*,[7] e.g., problems arise due to abstraction and overparametrization. We are following rather than predicting the available spectral data. The simulation allows us the direct use of more realistic (and more complicated) functions for the description of intermolecular interaction than the Debye theory[14] of Eq. (1), which assumes an isotropic resistance to reorientation.

The time autocorrelation functions of primary interest to the various rotational spectroscopics now available are the functions which we shall denote by $\langle P_n(t)\rangle$, n being positive integral. These can be defined in a way analogous with the Legendre polynomials. For the vector $\mathbf{e}_B$,

$$\langle P_1(t)\rangle = \langle \mathbf{e}_B(t)\cdot \mathbf{e}_B(0)\rangle\,, \tag{2}$$

$$\langle P_2(t)\rangle = \tfrac{1}{2}\langle 3[\mathbf{e}_B(t)\cdot \mathbf{e}_B(0)]^2 - 1\rangle\,, \tag{3}$$

as usual. These are illustrated in Figs. 3–5 with and without $\mathbf{T}_{ext}$. Their qualitative features are familiarly nonexponential, the oscillations near $t = 0$ being more pronounced in the torque-on case. In contrast to Ullman's result,[4] the torque-on acf's ($n = 1$–6) decay more slowly for the rms torque ratio of Table I. This is the result, however, for $\langle \mathbf{e}_B(t)\cdot \mathbf{e}_B(0)\rangle$, which is an average of different components, shown in normalized form in

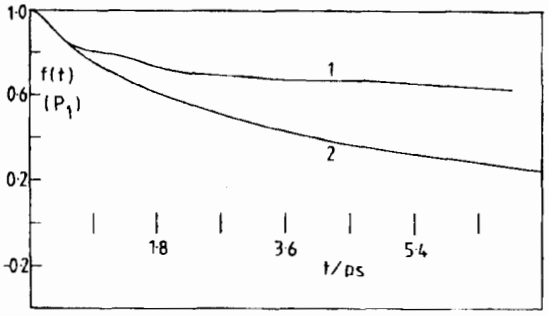

FIG. 3. Effect of torque on $\langle P_1(t)\rangle$. (1) Torque on; (2) torque off. Ordinate: $f(t) \equiv P_1(t)$; abscissa: time (ps).

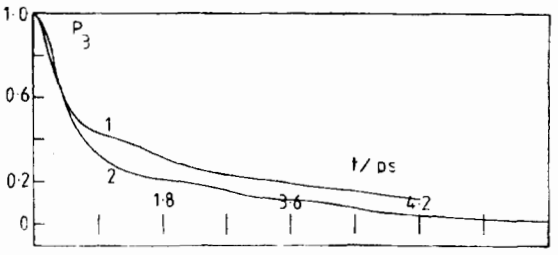

FIG. 5. As for Fig. 3, $\langle P_3(t)\rangle$.

Fig. 6. For different $\mathbf{T}_{ext}$, Ullman's results may well be supported. There is evidence in Fig. 4 that the torque-on $P_2(t)$ starts to fall faster but is slowed up further into the simulation, and similarly in Fig. 5 for $P_3(t)$.

Of interest to far infrared specialists[2,8] is the behavior under $\mathbf{T}_{ext}$ of $\langle \dot{\mathbf{e}}_B(t) \cdot \dot{\mathbf{e}}_B(0)\rangle$ which develops oscillations (Fig. 7). This means that the power absorption spectrum [$\alpha(\omega)$ in Np cm^{-1}] will sharpen and shift to higher frequencies. If the external torque is much larger than the internal torques, then the referee has pointed out that the orientational dynamics will become coherent (inhomogeneous) as in an ideal gas. Thus, one would expect the behavior observed in Fig. 7. However, we add that the torque-on far infrared peak frequency would be much higher than that of the ideal gas, even when observing the latter at very much higher temperatures. Because of the involvement of J in the strictly kinematic equation linking $\mathbf{e}_B$ to $\dot{\mathbf{e}}_B$, it seems that the far infrared spectrum would be more sensitive to changes of this kind than the dielectric loss, related to $\langle \mathbf{e}_B(t) \cdot \mathbf{e}_B(0)\rangle$ itself. The $\alpha(\omega)$ spectrum would be different along X, Y, and Z if it were possible to measure it this way.

The effect on the angular momentum autocorrelation function (Fig. 8) is to make this more oscillatory and to develop the anisotropy considerably. This is an acf which is very difficult to extract spectrally (spin–rotation NMR line broadening) but is at the same time central to the phenomenological theory of rotational diffusion, based[8] on the Langevin equation or forms of the Mori equation. Computer simulation seems therefore to be a particularly useful guide in the case of this acf simply because it *guides* the theoreticians in their search for a general description, and tests the many assumptions inherent in the data reduction of the spectroscopists. The angular momentum acf from Eq. (1) is a pure exponential in the torque-off case which is not so in Fig. 8. Therefore, Eq. (1) can hardly be a sound description in the torque-on case without further elaboration. In consequence, Eq. (1) is not a sound description of liquid-crystal spectra in the complete frequency range[8] from static to THz (far infrared). It is relatively uninformative in the context of molecular dynamics to cover this range only partially for either isotropic or anisotropic liquids.

Of interest in this context are the "response functions" or mixed acf's: $\langle \mathbf{J}(t) \cdot \mathbf{T}_q(0)\rangle$ and $\langle \mathbf{T}_q(t) \cdot \mathbf{J}(0)\rangle$, which using the relation $\mathbf{T}_q = \dot{\mathbf{J}}$ may be written as $\langle \mathbf{J}(t) \cdot \dot{\mathbf{J}}(0)\rangle$ and $\langle \dot{\mathbf{J}}(t) \cdot \mathbf{J}(0)\rangle$. The theory of classical autocorrelation functions implies that these two functions should be mirror images, and the simulation (Fig. 9) corroborates this expectation. This also underlines the fact that running time averages and ensemble averages are equivalent in the simulation in the presence of $\mathbf{T}_{ext}$. In Fig. 9 we illustrate the fact that running time averages over 10 and 20 ps provides the same result. This implies that the basic Langevin structure should be replaced by one of the type discussed by Evans and Davies[15]:

$$\mathbf{A} = \begin{bmatrix} \mathbf{J} \\ \dot{\mathbf{J}} \end{bmatrix}$$

The column vector **A** then obeys the equation

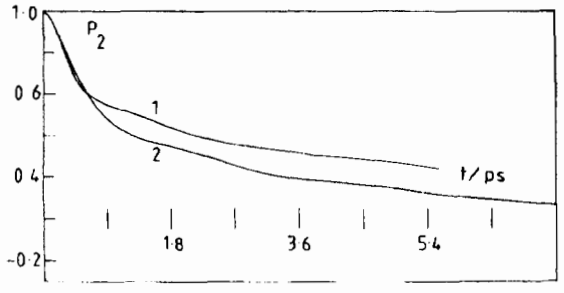

FIG. 4. As for Fig. 3, $\langle P_2(t)\rangle$. Order parameter = 0.585.

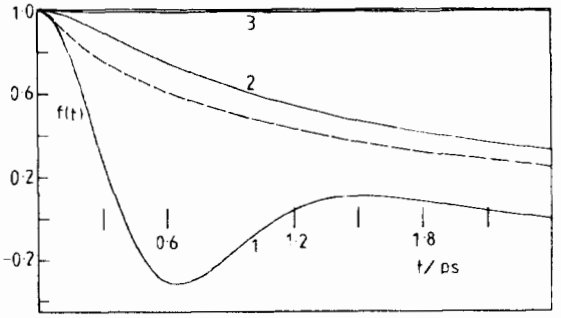

FIG. 6. Anisotropy of $\langle \mathbf{e}_B(t) \cdot \mathbf{e}_B(0)\rangle$. (1) $\langle e_{BX}(t)\, e_{BX}(0)\rangle / \langle e_{BX}^2(0)\rangle$; (2) Y component; (3) Z component. – – –, $\langle \mathbf{e}_B(t) \cdot \mathbf{e}_B(0)\rangle / \langle \mathbf{e}_B(0) \cdot \mathbf{e}_B(0)\rangle$. Ordinate and abscissa as for Fig. 3.

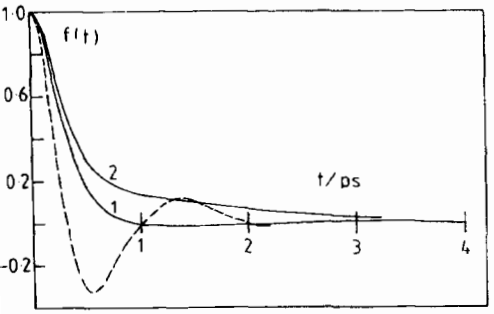

FIG. 7. (1) $\langle \dot{\mathbf{e}}_B(t)\cdot\dot{\mathbf{e}}_B(0)\rangle/\langle\dot{\mathbf{e}}_B(0)\cdot\dot{\mathbf{e}}_B(0)\rangle$, no torque. (2) $\langle \mathbf{J}(t)\cdot\mathbf{J}(0)\rangle/\langle\mathbf{J}(0)\cdot\mathbf{J}(0)\rangle$, no torque. - - - - - $\langle\dot{\mathbf{e}}_B(t)\cdot\dot{\mathbf{e}}_B(0)\rangle/\langle\dot{\mathbf{e}}_B(0)\cdot\dot{\mathbf{e}}_B(0)\rangle$, with torque. Ordinate and abscissa as for Fig. 3.

$$\frac{\partial p}{\partial t} = -\frac{\partial}{\partial \mathbf{A}}\cdot(\dot{C}_A C_A^{-1}\mathbf{A}p) + \frac{1}{2}\frac{\partial}{\partial \mathbf{A}}\cdot\left[C_A\frac{d}{dt}(M^{-1})C_A^T\frac{\partial p}{\partial \mathbf{A}}\right], \tag{4}$$

which is a generalization of the Fokker–Planck equation intended to deal with non-Markovian but Gaussian statistics. Further generalizations are possible following Grigolini and co-workers[2,7] to deal with non-Markovian *and* non-Gaussian statistics.

In Eq. (4), $p(\mathbf{A}(t),\mathbf{A}(0);t)$ is a conditional probability density governing the evolution of the complete column vector $\mathbf{A}$ with time. C_A is a matrix of autocorrelation functions and M is similarly defined. The superscript T denotes transposition of the matrix in the usual way.

The simulated response functions are accurate mirror images of each other, so that the system is statistical ergodic and stationary in time. The absolute magnitude of each function is comparable with that of $\langle\mathbf{J}(t)\cdot\mathbf{J}(0)\rangle$ or $\langle\dot{\mathbf{J}}(t)\cdot\dot{\mathbf{J}}(0)\rangle$. The effective equation of motion for theories of the dielectric/far infrared (zero-THz) spectrum should therefore be extended, specifically in the absence of external perturbation, from the generalized Langevin equation

$$\dot{\mathbf{J}}(t) - i\Omega_J\mathbf{J}(t) + \int_0^t d\tau\,\phi_J(t-\tau)\mathbf{J}(\tau) = \mathbf{F}_J(t)\ . \tag{5}$$

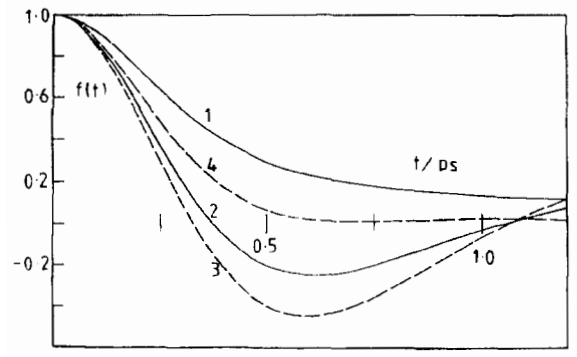

FIG. 8. (1) $\langle\mathbf{J}(t)\cdot\mathbf{J}(0)\rangle/\langle\mathbf{J}(0)\cdot\mathbf{J}(0)\rangle$, no torque. (2) Same function with torque. (3) $\langle J_X(t)J_X(0)\rangle/\langle J_X^2(0)\rangle$. (4) Y component. Ordinate and abscissa as for Fig. 3.

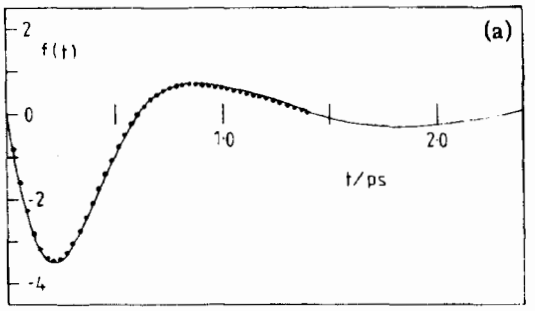

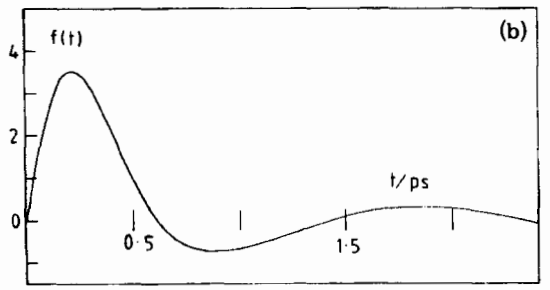

FIG. 9. (a) $\langle\mathbf{J}(t)\cdot\dot{\mathbf{J}}(0)\rangle/\langle\mathbf{J}(0)\cdot\mathbf{J}(0)\rangle$ constructed using a running time average over a total span of 20 ps. (o) The same with a span of 10 ps as a check on stability. (b) $\langle\dot{\mathbf{J}}(t)\cdot\mathbf{J}(0)\rangle/\langle\mathbf{J}(0)\cdot\mathbf{J}(0)\rangle$, which is, as it should be analytically, the mirror image of Fig. 9(a). Ordinate and abscissa as in Fig. 3.

(formally valid for asymmetric top diffusion) to the matrix equation [in Eq. (5), Ω_J is the Mori resonance operator, which vanishes for autocorrelations of the type we are dealing with here. ϕ_J is a matrix of memory functions and $\mathbf{F}_J$ is the vector first defined by Mori in a dynamical subspace created using projection operators]

$$\frac{d}{dt}\begin{bmatrix}\mathbf{J}(t)\\ \dot{\mathbf{J}}(t)\end{bmatrix} - i\Omega_{JJ}\begin{bmatrix}\mathbf{J}(t)\\ \dot{\mathbf{J}}(t)\end{bmatrix} + \int_0^t d\tau\,\phi_{JJ}(t-\tau)\begin{bmatrix}\mathbf{J}(\tau)\\ \dot{\mathbf{J}}(\tau)\end{bmatrix} = \begin{bmatrix}\mathbf{F}_J(t)\\ \dot{\mathbf{F}}_J(t)\end{bmatrix}\ . \tag{6}$$

Both these analytical equations are difficult to solve or interpret because the nonlinear Euler equations have to be cast into linear integrodifferential form.

In the presence of a strong external perturbation these equations *are modified fundamentally* as described by Ferrario and Grigolini,[7] and the methods of solution then involve *time ordered* exponential operators. However, when we consider liquid-crystalline alignment by application of a *weak* external field to a nematic sample, for example, the analytical task becomes less formidable; equations such as Eq. (1) can be used in the simplest case. It should be noted that the Hamiltonian with an applied torque (magnetic or electric) breaks parity symmetry and new cross correlations should become observable on a multiparticle level, and perhaps also on a single-particle level, although this is not entirely clear at present. If the molecules are optically active, then single-particle cross correlations should certainly appear in the presence of an external torque. Pentatomic algorithms are now available to investigate this

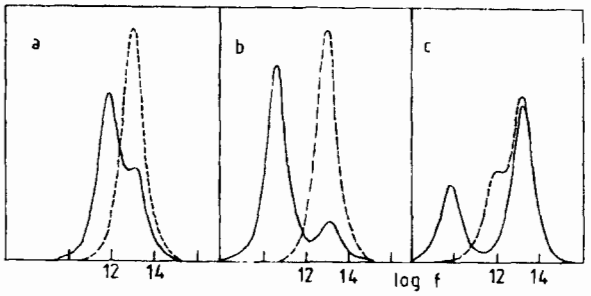

FIG. 10. (a), (b), and (c). Dielectric loss spectra for parameters β_ω, $\beta_{\dot\omega}$, $\beta_{\omega\dot\omega}$, and $\beta_{\dot\omega\omega}$ chosen to illustrate their effect on the Debye curve.

in detail. However, it is important to note that the case of column vectors $\begin{bmatrix} \mathbf{J} \\ \dot{\mathbf{J}} \end{bmatrix}$ instead of just the single component vector $\mathbf{J}$ in the equations of motion may lead to fundamental spectral changes *even in the absence of external perturbations*. If, for the sake of argument, the rotational motion is constrained to a plane, in order to linearize the Euler equations, then in the simplest case the Langevin equation would evolve from

$$\dot{\boldsymbol{\omega}}(t) = -\beta\boldsymbol{\omega}(t) + \boldsymbol{\Gamma}(t) \tag{7}$$

to

$$\frac{d}{dt}\begin{bmatrix} \boldsymbol{\omega}(t) \\ \dot{\boldsymbol{\omega}}(t) \end{bmatrix} = -\begin{bmatrix} \beta_\omega & \beta_{\omega\dot\omega} \\ \beta_{\dot\omega\omega} & \beta_{\dot\omega} \end{bmatrix}\begin{bmatrix} \boldsymbol{\omega}(t) \\ \dot{\boldsymbol{\omega}}(t) \end{bmatrix} + \begin{bmatrix} \boldsymbol{\Gamma}(t) \\ \dot{\boldsymbol{\Gamma}}(t) \end{bmatrix} , \tag{8}$$

i.e., the friction coefficient β evolves into a matrix of coefficients. Using the relation

$$\langle \dot{\mathbf{J}}(t)\cdot\mathbf{J}(0)\rangle = -\langle \dot{\mathbf{J}}(0)\cdot\mathbf{J}(t)\rangle$$
$$= -\frac{d}{dt}\langle \mathbf{J}(t)\cdot\mathbf{J}(0)\rangle ,$$

there are relations between the coefficients β_ω, $\beta_{\omega\dot\omega}$, $\beta_{\dot\omega\omega}$, and $\beta_{\dot\omega}$, so that there are no more than two loose parameters. Solving Eq. (8) for specified values of these parameters, chosen for the sake of illustration only, produces the dielectric spectrum of Fig. 10, which can be considerably split and shifted provided that $\beta_\omega\beta_{\dot\omega} \neq \beta_{\omega\dot\omega}\beta_{\dot\omega\omega}$. This comes from the fact that the angular velocity acf is now defined by

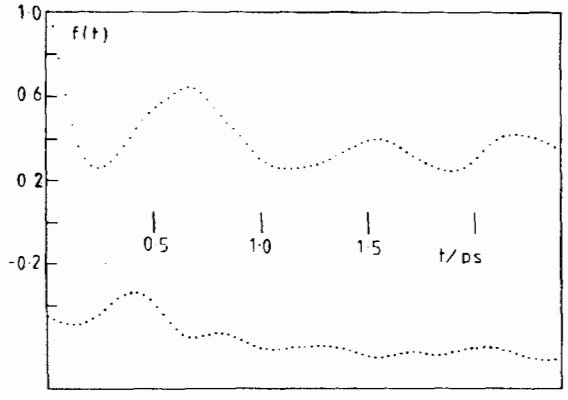

FIG. 11. $\langle J^6(t)\,v^6(0)\rangle/\langle J^6(0)\,v^6(0)\rangle$ with applied torque. Ordinate and abscissa as in Fig. 3.

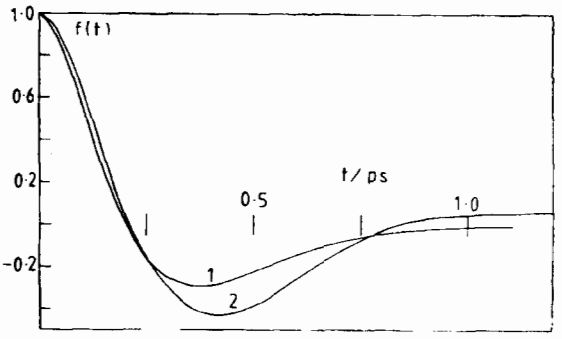

FIG. 12. $\langle \mathbf{T}_q(t)\cdot\mathbf{T}_q(0)\rangle/\langle \mathbf{T}_q(0)\cdot\mathbf{T}_q(0)\rangle$, the molecular torque acf. (1) No external torque; (2) with external torque. Ordinate and abscissa as in Fig. 3.

$$\langle \boldsymbol{\omega}(t)\cdot\boldsymbol{\omega}(0)\rangle/\langle \boldsymbol{\omega}(0)\cdot\boldsymbol{\omega}(0)\rangle$$
$$= \mathcal{L}_a^{-1}\left[\frac{p+\beta_{\dot\omega}}{(p+\beta_\omega)(p+\beta_{\dot\omega}) - \beta_{\omega\dot\omega}\beta_{\dot\omega\omega}}\right] - \mathcal{L}_a^{-1}(p+\beta_\omega)^{-1} ,$$

when $\beta_{\omega\dot\omega} = 0$. This is the classical Debye result valid in two dimensions for the rotating asymmetric top, and in three dimensions for isotropic rotational diffusion.

The new problems which follow from a proper consideration of $\langle \dot{\mathbf{J}}(t)\cdot\mathbf{J}(0)\rangle = -\langle \dot{\mathbf{J}}(0)\cdot\mathbf{J}(t)\rangle$ are therefore numerous. The simulation may be said to have isolated the role played by response functions of this kind. These considerations lead to the conclusion that use of column vectors instead of just the single component J can lead to important spectral changes even in the absence of perturbation and anisotropy. We extrapolate and predict that these vectors will be important in the analytical theory of liquid anisotropy, where symmetry constraints on the existence of mixed autocorrelation functions are less stringent, due to the presence of a symmetry breaking field.[16]

We have searched for other mixed autocorrelation functions but those of the type $\langle \dot{X}(t)X(0)\rangle$ are by far the most pronounced in the torque-on and torque-off cases. For economic reasons we have not tried longer runs in an attempt to define properly the behavior of functions such as $\langle Y(t)X(0)\rangle$, where Y and X stand for vectors of different type. Mixed autocorrelation functions of this type can be illustrated in moment form as in Fig. 11. The analytical theory of such moment functions is relatively undeveloped, and should be based, naturally, on the same equations of motion as for $\langle \mathbf{J}(t)\cdot\mathbf{J}(0)\rangle$ and $\langle \mathbf{v}(t)\cdot\mathbf{v}(0)\rangle$ themselves.

Interestingly, the external torque $\mathbf{T}_{ext}$ affects the torque acf $\langle \mathbf{T}_q(t)\cdot\mathbf{T}_q(0)\rangle$ itself to a smaller degree than the angular momentum acf which in turn is less affected in terms of the anisotropy than the orientation acf's $\langle \mathbf{e}_B(t)\cdot\mathbf{e}_B(0)\rangle$ and $\langle \dot{\mathbf{e}}_B(t)\cdot\dot{\mathbf{e}}_B(0)\rangle$. The torque acf with and without $\mathbf{T}_{ext}$ is illustrated in Fig. 12.

V. DISCUSSION

The above results illustrate an attempt to supplement our analytical knowledge of liquid phase anisotropy. We have not been concerned with reproducing some available experimental data (which are sparse in the ps interval)

but to simulate some functions more or less fundamental to the evaluation of the available phenomenological ideas. Central to this aim is the simulation of the angular momentum acf of diffusing asymmetric tops.

The computer enables us to use an external torque of arbitrary strength and origin with a minimum of mathematical elaboration. In our opinion it would be less justifiable to use the molecular dynamics method with more complicated mechanisms of anisotropy induction without attempting to simulate a real system, such as water. The most intense field strengths available experimentally are probably pulses of electromagnetic radiation, and an obvious target for computer simulation would be with an external laser field of far infrared frequency. The field causing the anisotropy would itself be modulated by the rotational motion of the molecules, providing some extra insights. This is possible experimentally using relatively low intensity carcinotrons in the GHz–THz range of frequencies.

Another interesting exercise would be to vary the external torque strength in an attempt to see whether the development of anisotropy shows any sign of a discontinuity, indicating a phase change, i.e., to see whether an intense enough field makes a "mesophase" out of a normally isotropic phase. A positive result here would depend on the definition used for a mesophase. In many respects the large anisotropy reported in this paper for e_B might lead us to classify the molecular dynamics sample in the torque-on case as a mesophase. This is speculative until results are available with different T_{ext}.

VI. CONCLUSIONS

(1) The molecular dynamics method can be extended straightforwardly to deal with the difficult analytical problems of anisotropic liquids.

(2) The angular momentum acf becomes more oscillatory on application of an external torque, and analytical theories based on an experimental acf are not valid in the ps time range.

(3) A torque breaks parity symmetry and the extra correlations appearing in the liquid could be investigated by a simulation of this kind.

(4) We have exemplified the use of molecular dynamics simulation as an investigative theoretical aid rather than as a directly analytical approach to available experimental data.

(5) Translational, as well as rotational, molecular dynamical properties are affected by the torque.

ACKNOWLEDGMENTS

SRC is acknowledged for financial support. Mauro Ferrario is thanked for useful discussion.

[1]C.J.F. Bottcher and P. Bordewijk, *Theory of Electric Polarization* (Elsevier, Amsterdam, 1978).
[2]M. W. Evans, W. T. Coffey, G. J. Evans, and P. Grigolini, *Molecular Dynamics* (Wiley/Interscience, New York, in press).
[3]H. Bénoit, Ann. Phys. (Paris) 6, 561 (1951); J. Chim. Phys. 49, 517 (1951).
[4]R. Ullman, J. Chem. Phys. 56, 1869 (1972).
[5]W. T. Coffey and B. V. Paranjape, Proc. R. Irish Acad. Sect. A 78, 17 (1976).
[6]P. L. Nordio, G. Rigatti, and U. Segre, J. Chem. Phys. 56, 2117 (1972).
[7]P. Grigolini and M. W. Evans, J. Chem. Soc. Faraday Trans. 2 76, 761 (1980); P. Grigolini, M. Ferrario, and M. W. Evans, *ibid.* 76, 542 (1980); P. Grigolini and M. Ferrario, J. Math. Phys. 20, 2567 (1979).
[8]M. W. Evans, A. R. Davies, and G. J. Evans, Adv. Chem. Phys. 44, 255 (1980).
[9]K. Singer (private communication).
[10]A. Rahman, Phys. Rev. Sect. A 136, 405 (1964).
[11]B. J. Berne and G. D. Harp, Adv. Chem. Phys. 17, 63 (1970).
[12]M. W. Evans, M. Ferrario, and P. Grigolini, Z. Phys. B 41, 165 (1981).
[13]C. Brot, G. Bossis, and C. Hesse-Bezot, Mol. Phys. 40, 1053 (1980).
[14]P. Debye, *Polar Molecules* (Chemical Cat. Co., New York, 1929).
[15]A. R. Davies and M. W. Evans, Mol. Phys. 35, 857 (1978).
[16]B. J. Berne and R. Pecora, *Light Scattering with Applications to Physics, Chemistry and Biology* (Wiley/Interscience, New York, 1976).